Comparison between GEANT4 and MCNP for well logging applications

Geoffrey Varignier, Valentin Fondement, Cédric Carasco, Johann Collot, Bertrand Pérot, Thomas Marchais, Pierre Chuilon, Emmanuel Caroli, Mai-Linh Doan

Comparison between GEANT4 and MCNP for well logging applications

Geoffrey Varignier[1,*], Valentin Fondement[2], Cédric Carasco[2], Johann Collot[3], Bertrand Pérot[2], Thomas Marchais[2], Pierre Chuilon[1], Emmanuel Caroli[1], Mai-Linh Doan[4]

[1]TotalEnergies, France
[2]CEA, France
[3] LPSC-IN2P3, France
[4]Univ. Grenoble Alpes, Univ. Savoie Mont Blanc, CNRS, IRD, Univ. Gustave Eiffel, ISTerre, France
(*) geoffrey.varignier@totalenergies.com

***Abstract*— MCNP and GEANT4 are two reference Monte Carlo nuclear simulators, MCNP being the standard in the Oil & Gas nuclear logging industry. While performing a simulation benchmark of these two software for the purpose of "Cased Hole" wellbore evaluation, discrepancies between MCNP and GEANT4 were observed: computational experiments were performed first in a theoretical and simplified environment using spherical models, then in a more realistic "Open Hole" wellbore context with simplified logging tools. Results of this comparison show an excellent overall agreement for gamma-gamma physics and an acceptable agreement for neutron-neutron physics. However, the agreement for neutron-gamma physics is satisfactory only for certain lithologies and energy windows, but not acceptable for other operating conditions. These results need to be put in perspective with the current use of nuclear simulation in the logging industry. Indeed, wellbore evaluations rely on charts simulated with Monte Carlo codes in various contexts. In the case of radially heterogeneous environments such as "Cased Hole" wellbores, nuclear simulations are mandatory to precisely determine the radial sensitivity of logging tools via the so-called sensitivity functions. The feasibility of wellbore inversion relies on the physical validity of such sensitivity functions obtained from nuclear simulations. This MCNP vs. GEANT4 benchmark was conducted with the perspective to secure the physical fundamentals used for building the sensitivity functions of logging tools.**

***Keywords*— Well logging, Monte-Carlo modeling, MCNP, GEANT4, Gamma-Gamma, Neutron-Neutron, Neutron-Gamma, Sensitivity function, Nuclear logging probes.**

I. INTRODUCTION

Nuclear logging tools have been used in the oil and gas industry for over the last 70 years, mainly to characterize formation reservoirs and to monitor the hydrocarbon fraction in the close vicinity of the wellbore during production. Many logging probes based on different nuclear physics are frequently used for data acquisition. Once calibrated, the data acquired along the wellbore are interpreted into some parameters of interest, such as porosity, density, water saturation, etc.

To understand the sensitivity of nuclear measurements to the target properties and convert them to quantitative ones, the oil industry started using recurrently Monte Carlo nuclear simulations [11]. It enables the 3D modeling of particle interactions with matter through a stochastic approach. Trajectories of millions of particles (neutrons or gamma) are simulated simultaneously. Their interactions with the logging tool itself, borehole fluid, casing, cement and formation are calculated using the principles of nuclear physics. Particles heading to the detectors are counted and their spectra analyzed similarly to what occurs in any logging tool.

Oilfield Services companies and Oil&Gas companies usually use MCNP (Monte Carlo N-Particle) computer code to model the logging tools response to various wellbore contexts. This software is considered standard in the Oil&Gas industry [1]. MCNP is a Monte Carlo nuclear simulation code written in Fortran 90 and C, developed by the Los Alamos National Laboratory (USA). Being developed by a US institution, MCNP is not available all over the world. An alternative to MCNP is GEANT4 (GEometry ANd Tracking) [10], which is another Monte Carlo nuclear simulation toolkit written in C++ and developed by the CERN agency. Although originally developed for high-energy physics, it has been extended to applications in low-energy physics.

The goal of nuclear simulations is to characterize the relationship between the nuclear measurements and the wellbore components: reservoir properties, as well as completion, production fluids, steel casings, and cement in case the well is cased (i.e. a steel casing is cemented to the wellbore wall). In such a configuration, the number of unknowns is so large (casing and cement thicknesses and grades, tubing centralization, etc.) that the inverse problem requires the combination of various physics (with nuclear and non-nuclear probes) covering compatible radii of investigation. Exact knowledge of the detectors sensitivity for all nuclear probes is then essential and obtained from nuclear simulations.

The industry standard is to run MCNP with biasing techniques [15][16][17]. However, the fundamental of this assumption needs to be revised when applied to the radially heterogeneous "Cased Hole" domain with independent numerical calculations using MCNP and GEANT4. Prior to validate the concept of sensitivity function for "Cased Hole"

environment, discrepancies between both software have been evaluated in this paper without biasing and variance reduction techniques to highlight discrepancies observed between MCNP and GEANT4 and present quantitative results from a comparison in a logging environment. First calculations are performed with a theoretical and simplified spherical model and then in a more realistic "Open Hole" model using simplified logging tools such as Litho-Density, Neutron-Porosity and Carbon/Oxygen.

II. GEOMETRY AND VISUALIZATION

Figure 1 shows the spherical model allowing for a first comparison between the codes, displayed with the MCNP Vised visualization software. It consists of a 22.9 cm radius sphere surrounded by a spherical NaI(Tl) or 3He detection volume with an external radius of 34.9 cm and a thickness of 3 cm. The inner sphere is composed of a pure material commonly encountered in Geoscience problems (carbon ; oxygen ; calcium ; magnesium ; silicon ; hydrogen).

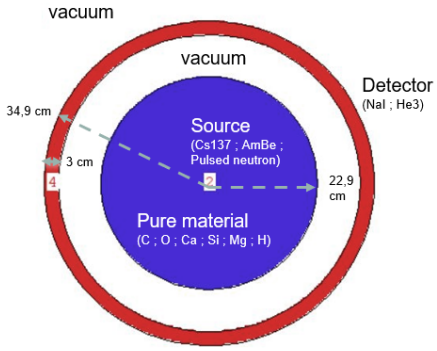

Fig. 1. Spherical model displayed using Vised.

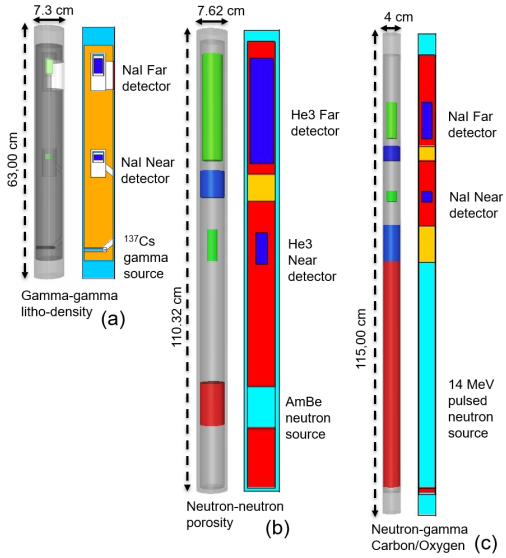

Fig. 2. Gamma-gamma density (a), neutron-neutron porosity (b) and neutron-gamma Carbon/Oxygen (C/O) (c) generic logging tools models displayed using EDGE (left) and Vised (right).

On the GEANT4 side, visualization software such as EDGE can be used to build geometries and export them to GDML format [4][22], to obtain views such as the well logging tool shown in Figure 2. Generic logging tools models are very simplified and supposed to mimic the physical response of commercial logging tools operated by oilfield services companies. These models use main elements of logging tools such as detectors, shields and sources. Key parameters such as source-detectors distances, detectors and shield volumes and tool dimensions are close to real logging tools. Generic logging tools models were developed by the Austin University [14][15].

Figure 3 shows a 3D model of a neutron-gamma C/O logging tool, a pure lithology and a 200 mm water filled borehole. 3D geometry modeling capabilities of MCNP and GEANT4 are comparable and external software such as Vised, or EDGE, can be used to check the model in detail.

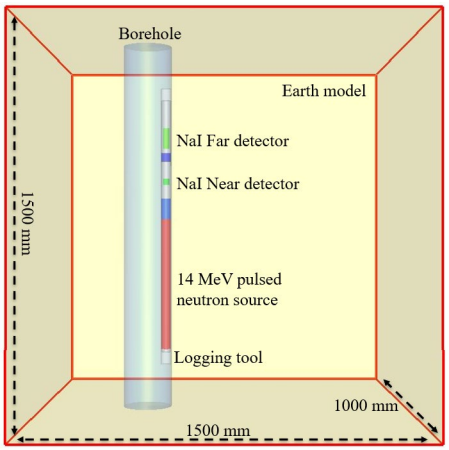

Fig. 3. Neutron-gamma C/O generic logging tools in a water filled borehole model displayed using EDGE. The well is filled with fresh water and the Earth model is composed of a pure lithology at 20 pu (porosity unit) such as sandstone (SiO_2), limestone ($CaCO_3$) or dolomite ($CaMg(CO_3)_2$). Rock porosity is fully saturated with fresh water.

III. GAMMA-GAMMA MEASUREMENT

Gamma-gamma measurement consists in measuring with a NaI(Tl) detector the gamma spectrum originating from a ^{137}Cs radioactive source of mono-energetic 661.7 keV gamma rays, mostly after their Compton scattering in the rock formation [13]. The Compton continuum starting at the initial energy 661.7 keV is measured using a "Hard window" from 540 keV down to about 150 keV, where the Compton interaction dominates. In the Geosciences field, this continuum is used to derive the formation density. On the other hand, the photoelectric effect (PEF) is measured using a "Soft window" between 60 keV and approximately 100 keV. The "Soft window" contains information about the rock mineralogy. To compensate for the photoelectric contribution in the "Hard window", a lithological matrix correction is performed based on PEF.

Gamma-gamma measurements are simulated in MCNP with the F8 pulse height tally, which provides the histogram of photon energy deposits in a detector (i.e. the gamma spectrum), per source particle. The F8 spectrum being normalized to one source particle [2], it is scaled with the number of particles simulated in GEANT4 to allow a quantitative comparison. Gamma-gamma measurements are simulated in GEANT4 by scoring in *"SteppingAction.cc"*, the distribution of energies deposited by gamma rays entering in the NaI detector.

Figure 4 shows six gamma-gamma measurement spectra in a spherical model for six pure chemical elements.

Tables I and II give the total counts integrated in the Hard and Soft windows for a spherical model and show a maximum discrepancy of 4.0% for calcium.

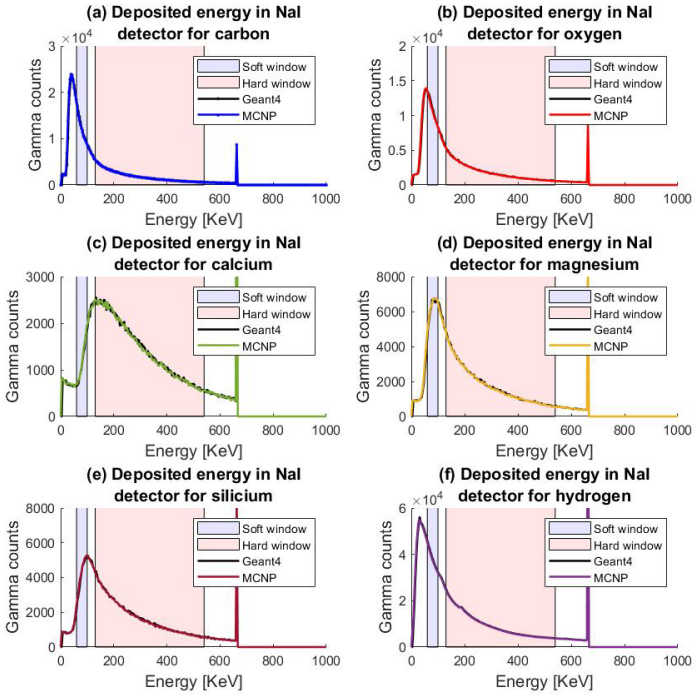

Fig. 4. Simulated gamma-gamma spectra with a spherical model, a ^{137}Cs gamma source, a NaI detector and 6 pure materials. Five materials have a density of 2.71 g/cm3 (C, O, Ca, Mg, Si), and due to its large number of nuclei per volume unit, one material has a density of 0.5 g/cm3 (H).

TABLE I. SOFT WINDOW TOTAL COUNTS OF GAMMA-GAMMA MEASUREMENTS IN A SPHERICAL MODEL FOR SIX PURE ELEMENTS.

Gamma-Gamma density measurements NEAR detector in Soft window			
	Carbon	Oxygen	Calcium
Counts MCNP	147622	128578	14932
Counts GEANT4	151926	131276	14331
GEANT4/MCNP	2,9%	2,1%	4,0%

Gamma-Gamma density measurements NEAR detector in Soft window			
	Magnesium	Silicium	Hydrogen
Counts MCNP	74436	50755	453733
Counts GEANT4	73381	48942	461870
GEANT4/MCNP	1,4%	3,6%	1,8%

TABLE II. HARD WINDOW TOTAL COUNTS OF GAMMA-GAMMA MEASUREMENTS IN A SPHERICAL MODEL FOR SIX PURE ELEMENTS.

Gamma-Gamma density measurements NEAR detector in Soft window			
	Carbon	Oxygen	Calcium
Counts MCNP	192248	190119	150395
Counts GEANT4	194282	192895	152209
GEANT4/MCNP	1,1%	1,5%	1,2%

Gamma-Gamma density measurements NEAR detector in Soft window			
	Magnesium	Silicium	Hydrogen
Counts MCNP	184011	177965	983344
Counts GEANT4	186786	180601	1002273
GEANT4/MCNP	1,5%	1,5%	1,9%

Figure 5 shows six gamma-gamma density measurement spectra of a generic logging tool with two detectors (NEAR and FAR) in a 200 mm diameter borehole and for three rock compositions. On Fig 5, a Gaussian Energy Broadening (GEB) has been performed on each spectrum.

Tables III and IV give the total counts integrated in the Hard and Soft windows for a litho-density logging tool model and show maximum discrepancies of 4.3% for the NEAR detector and 11.3% for the FAR detector.

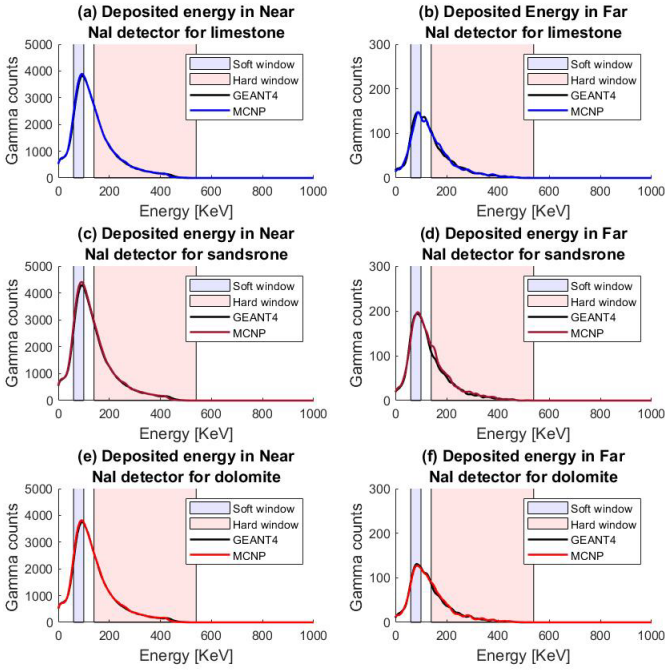

Fig. 5. Simulated gamma-gamma measurements spectra with a lithology-density generic logging tool model, a ^{137}Cs gamma source, two NaI detectors and three different rocks at 20 pu (porosity unit): a 2.368 g/cm3 limestone (a, b), a 2.323 g/cm3 sandstone (c, d), and a 2.496 g/cm3 dolomite (e, f).

Discrepancies are larger between MCNP and GEANT4 using the logging tool model compared to the spherical model, which could be due to the larger number of interactions along the particles random walk. Moreover, the smaller number of counts induce larger calculation statistical uncertainties. Simulations in MCNP and GEANT4 have been performed without biasing techniques to compare the analog gamma transport. Variance reduction techniques could be useful for gamma-gamma density measurements to improve statistics. In Geosciences, the density is mainly based on the FAR detector. Even if the absolute number of counts is lower compared to the NEAR detector, the measurement is more representative of the geological formation because of the larger depth of investigation. NEAR detector is used to correct the density measurement of environmental effects such borehole and mudcake effects. Nevertheless the overall agreement between GEANT4 and MCNP is satisfactory for gamma-gamma physics, as already reported in other benchmarks and shows discrepancies lower than 12% [23].

TABLE III. SOFT WINDOW TOTAL COUNTS OF GAMMA-GAMMA MEASUREMENTS IN A DENSITY GENERIC LOGGING TOOL MODEL WITH TWO DETECTORS IN THREE ROCK COMPOSITIONS AT 20 PU.

Gamma-Gamma density measurements NEAR detector in Soft window			
	Limestone	Sandstone	Dolomite
Counts MCNP	37376	42976	37153
Counts GEANT4	35981	41134	35903
GEANT4/MCNP	3,7%	4,3%	3,4%

Gamma-Gamma density measurements FAR detector in Soft window			
	Limestone	Sandstone	Dolomite
Counts MCNP	1372	1975	1274
Counts GEANT4	1446	1989	1308
GEANT4/MCNP	5,4%	0,7%	2,7%

TABLE IV. HARD WINDOW TOTAL COUNTS OF GAMMA-GAMMA MEASUREMENTS IN A DENSITY GENERIC LOGGING TOOL MODEL WITH TWO DETECTORS IN THREE ROCK COMPOSITIONS AT 20 PU.

Gamma-Gamma density measurements NEAR detector in Hard window			
	Limestone	Sandstone	Dolomite
Counts MCNP	54709	57813	51890
Counts GEANT4	54419	56674	51579
GEANT4/MCNP	0,5%	2,0%	0,6%

Gamma-Gamma density measurements FAR detector in Hard window			
	Limestone	Sandstone	Dolomite
Counts MCNP	2068	2422	1706
Counts GEANT4	2004	2149	1625
GEANT4/MCNP	3,1%	11,3%	4,7%

IV. NEUTRON-NEUTRON MEASUREMENT

The neutron-neutron measurement consists in counting backscattered neutrons originating from an Americium-Beryllium (AmBe) radioactive spectral neutron source with an ^{3}He detector [13]. It is mainly sensitive to the hydrogen content of the rock because of the large elastic scattering and radiative capture cross sections of hydrogen nuclei. The transform of hydrogen content into porosity is strongly linked to the physicochemical nature of fluids or gas (fresh water, brine, hydrocarbon liquid or gas, CO_2). The other chemical elements like C, O, or Ca have a significant impact on neutron slowing down and capture only at very low porosity (i.e. a rock formation porosity close to 0 pu), inducing variations in the total number of counts according to rock density and mineralogy [6][7].

Neutron-neutron measurements are simulated in MCNP with the F4 tally, which is the average flux of neutron particles passing through a cell convoluted with the N°103 nuclear reaction cross section corresponding to the ^{3}He(n,p)^{3}H absorption reaction that creates the signal in the ^{3}He counters. The result obtained with MCNP is multiplied by the detector volume and the number of particles simulated in GEANT4 to allow a quantitative comparison. The neutron-neutron measurement is simulated in GEANT4 by scoring the number of ^{3}He(n,p)^{3}H reactions in *"SteppingAction.cc"*.

Figure 6 shows six neutron-neutron measurement spectra (neutron kinetic energy before inelastic nuclear interaction with helium 3 nuclei) in the spherical model for six pure chemical elements. Results obtained with MCNP are derived from statistical calculations and the abovementioned normalization, hence showing some counts inferior to one, whereas results obtained with GEANT4 are particle tracking calculations and show only counts superior to one.

Table V gives the total number of counts (number of ^{3}He(n,p)^{3}H reactions) for pure elements and shows a maximum discrepancy of 16.6% for hydrogen without molecular effects. Implementation of molecular effects allows reducing deviations of the total number of counts between MCNP and GEANT4 from 9.8% to 0.1% for carbon, and from 16.6% to 2.9% for hydrogen. Therefore, molecular effects on carbon and hydrogen will be implanted in next simulations. The maximum discrepancy is obtained with oxygen (7.0%) and magnesium (7.1%).

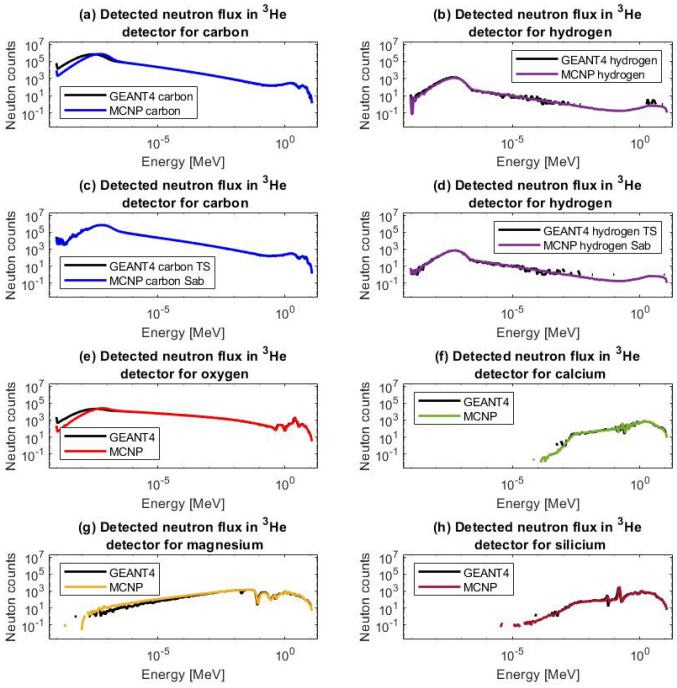

Fig. 6. Simulated neutron-neutron measurement spectra with a spherical model, an AmBe neutron source, a ^{3}He detector and six pure chemical elements. Five materials have a density of 2.71 g/cm3 (C, O, Ca, Mg, Si), and due to its large number of nuclei per volume unit, one material has a density of 0.5 g/cm3 (H). Graphics (c) and (d) show spectra with molecular effects on carbon and on hydrogen "Sab" for MCNP S(α,β) (grph.10t; lwtr.10t) and "TS" for GEANT4 Thermal Scattering (TS_C_of_Graphite; TS_H_of_Water).

TABLE V. TOTAL COUNTS OF NEUTRON-NEUTRON MEASUREMENTS IN A SPHERICAL MODEL FOR SIX PURE ELEMENTS (INCLUDING MOLECULAR EFFECTS FOR CARBON AND HYDROGEN).

Neutron-Neutron porosity measurements NEAR detector				
	Carbon with molecular effects	Carbon	Hydrogen with molecular effects	Hydrogen
Counts MCNP	17628283	18235366	14868	24662
Counts GEANT4	17644604	20019134	14430	28766
GEANT4/MCNP	0,1%	9,8%	2,9%	16,6%

Neutron-Neutron porosity measurements NEAR detector				
	Silicium	Oxygen	Calcium	Magnesium
Counts MCNP	26899	1178892	17635	81882
Counts GEANT4	27472	1261444	18029	76080
GEANT4/MCNP	2,1%	7,0%	2,2%	7,1%

Figure 7 shows six neutron-neutron porosity measurement spectra of a generic logging tool with two detectors (NEAR and FAR) in a 200 mm wellbore and for three rock compositions.

Table VI gives the total number of counts for compound materials and show a maximum discrepancy of 3.8% for the NEAR detector and 24.9% for the FAR detector.

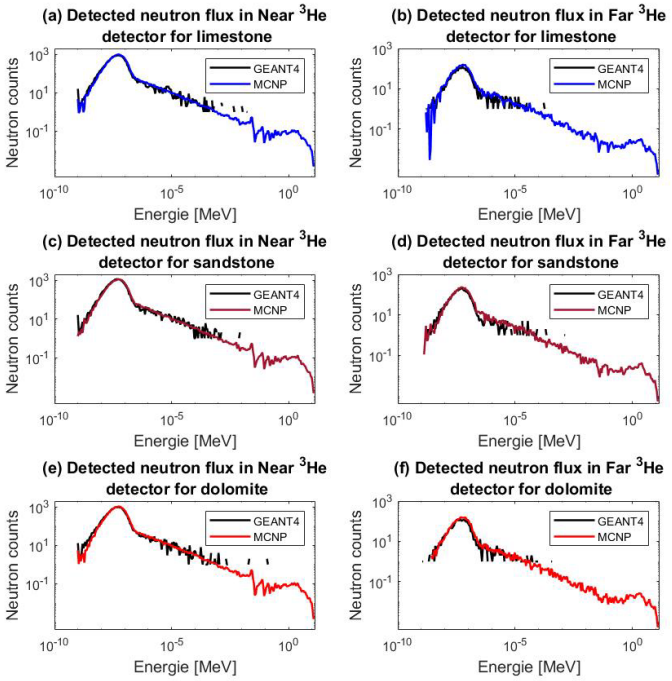

Fig. 7. Simulated neutron-neutron measurement spectra with a neutron-neutron porosity generic logging tool model, an AmBe neutron source, two ^{3}He detectors and three different rocks at 20 pu (porosity unit): a 2.368 g/cm3 limestone (a, b), a 2.3232 g/cm3 sandstone (c, d), and a 2.496 g/cm3 dolomite (e, f).

TABLE VI. TABLE OF TOTAL COUNTS INTEGRATED ON NEUTRON-NEUTRON MEASUREMENTS SPECTRA OF A POROSITY GENERIC LOGGING TOOL WITH TWO DETECTORS IN THREE ROCK COMPOSITIONS AT 20 PU.

Neutron-Neutron porosity measurements NEAR detector			
	Limestone	Sandstone	Dolomite
Counts MCNP	19994	23399	21420
Counts GEANT4	19227	23667	21164
GEANT4/MCNP	3,84%	1,15%	1,20%

Neutron-Neutron porosity measurements FAR detector			
	Limestone	Sandstone	Dolomite
Counts MCNP	3078	4521	3167
Counts GEANT4	2311	3922	2518
GEANT4/MCNP	24,93%	13,25%	20,49%

Using the particle tracking of GEANT4, one can identify nuclei that interacted with neutrons on their path from the Am-Be source to the detectors. In a wellbore model with a 20 pu sandstone lithology, 77% of the counts recorded in the NEAR detector involves interactions on hydrogen nuclei, and 80% for the FAR detector, the other interactions occurring on oxygen and silicon nuclei. In a well model with a 20 pu limestone or dolomite lithology, hydrogen account respectively for 69% and 66% of NEAR detector interactions, 72% and 70% of FAR detector interactions, the other interactions occurring on oxygen, carbon, calcium and magnesium nuclei. The large discrepancies between MCNP and GEANT4 in limestone and dolomite for the FAR detector could be explained by differences in neutron interaction cross sections of elements other than hydrogen. Indeed, for sandstone, in which interactions on hydrogen represent a larger fraction, the difference is smaller. The overall agreement between GEANT4 and MCNP for neutron-neutron physics is nevertheless still acceptable regarding borehole simulation objectives, with discrepancies under 25%.

V. NEUTRON-GAMMA MEASUREMENT

The neutron-gamma measurement consists in measuring the induced gamma spectrum originating from a 14 MeV mono-energetic pulsed neutron generator, with a NaI(Tl) detector [13]. In Geosciences, gamma spectra analysis simply consists in calculating the ratio of counts in two integration windows, the first one from ~ 3.2 MeV up to ~ 4.7 MeV focused on carbon gamma ray at 4.439 MeV (including its escape peaks at 3.928 and 3.417 MeV), the second one from ~ 4.8 MeV up to ~ 7.4 MeV focused on oxygen gamma ray at 6.129 MeV (and escape peaks 5619 and 5108 MeV). Neutron-gamma measurement, also called C/O measurement because it is based on the count ratio between carbon and oxygen windows, is particularly sensitive to quantity of water compared to quantity of oil, and thus to the hydrocarbon rock saturation.

Figure 8 shows four neutron-gamma measurement spectra in a spherical model for a pure carbon material. MCNP flux spectra (red lines) are identical and MCNP deposited energy spectra (blue lines) are also identical. GEANT4 flux and deposited energy spectra are computed with and without a pass band energy filter described below.

In the very particular geometry with a material sphere surrounded by a 4π spherical detector, multiple induced gamma rays generated in the same neutron history by successive inelastic scattering and radiative capture reactions can sum up in the detected gamma spectrum, introducing a single sum peak with an energy corresponding to the sum of the different gamma-ray energies (cf. figure 8, panels c and d, MCNP spectra). A two-step simulation is therefore mandatory to carry out a more realistic neutron-gamma C/O measurement, instead of the above single-step F8 simulation. In the first step, the MCNP F1 current tally scores gamma rays crossing the external surface of the carbon material sphere, the NaI detector cell being here filled with vacuum to avoid photon backscattering. In the second step, using the F1 calculation as a gamma spectral source at the entrance surface of the NaI detector, the F8 pulse height tally scores the energies deposited in the energy bins of the gamma spectrum.

In GEANT4, neutron inelastic scattering on carbon nuclei induces gamma rays over and bellow the main inelastic emission ray at 4.439 MeV that are not experimentally observed (cf. figure 8 a, c). Removing data of emission rays contained in *"G4NDL4.6\Inelastic\Gammas\z6.a12"*, except the ray at 4.439 MeV, does not allow to solve the problem. A pass band energy filter is added in "SteppingAction.cc" for neutron inelastic scattering on carbon nuclei to keep only gamma rays generated between 4 MeV and 5 MeV (cf. figure 8 b, d). Adding such filter allow GEANT4 results to be closer to MCNP [8][12][21]. Moreover, in GEANT4, within the same history as in MCNP, a neutron can create several inelastic gamma rays when scattering on different nuclei. The particle tracking simulation in a spherical geometry yields peaks on the gamma spectrum which are the sum of the energy of the gamma ray

generated by capture process and energies of multiple gamma rays generated by inelastic process (cf. figure 8, panel d, GEANT4 spectrum). It does not allow to simulate a realistic neutron-gamma C/O measurement and requires a two-step simulation. First, kinetic energies of gamma rays induced by neutrons entering in a vacuum filled detector are collected in "SteppingAction.cc" to build a spectral gamma source. Then, using the previous current spectrum as a source impinging the entrance surface of a NaI filled detector, deposited energies per energy bins are scored in "SteppingAction.cc".

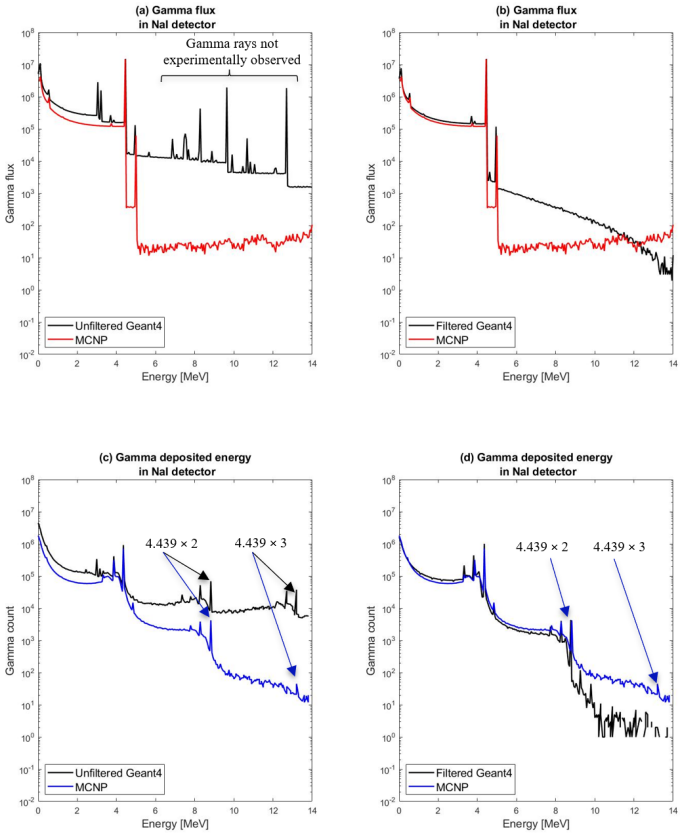

Fig. 8. Simulated neutron-gamma measurement spectra with a spherical model, a 14 MeV pulsed neutron source, an NaI detector and one pure carbon material. Spectra (a) and (b) show flux spectra of gamma rays entering in a NaI detector in cm-2 per 96×10^6 source particles. Spectra (c) and (d) show deposited energy spectra of gamma rays interacting in the NaI crystal.

Figure 9 shows three neutron-gamma measurement spectra in a spherical model for a pure carbon material. Two spectra (black and blue lines) are computed with a two times simulation. One spectrum (brown line) comes from experimental data of a 14 MeV pulsed neutrons source on a well-known sample of graphite [5][19]20].

The associated particle technique used to acquire the experimental spectrum allows recording only the 4.439 MeV inelastic scattering gamma ray of carbon (and its escape peaks also visible on the gamma spectrum). The 4.945 MeV due to radiative capture is not detected (cf. figure 9, brown line). The two-step simulations in MCNP and GEANT4 allows more realistic simulations of the gamma rays induced by fast and thermal neutrons on carbon nuclei.

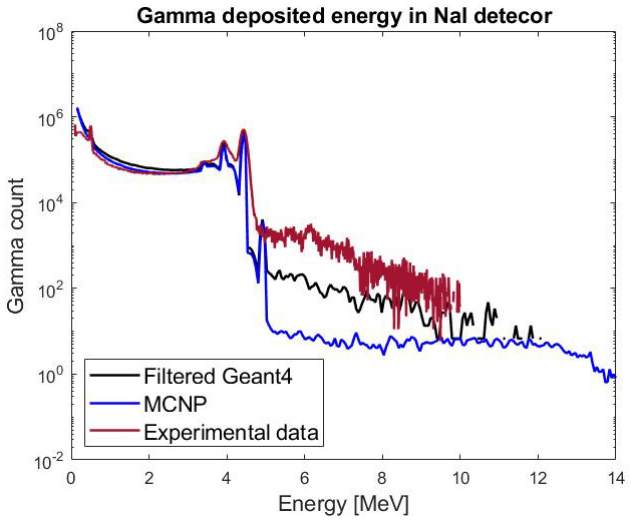

Fig. 9. Simulated and measured neutron-gamma spectra with a 14 MeV pulsed neutron source, a NaI detector and one pure carbon material. The calculated spectra are computed with two steps simulation in MCNP (blue line) and in GEANT4 (black line). The experimental spectrum (brown line) has been normalized to the amplitude of the main inelastic scattering carbon peak at 4.439 MeV of the MCNP spectrum to ease this qualitative comparison.

Figure 10 shows six neutron-gamma measurement spectra in a spherical model for six pure materials. No time decay analysis was implemented. Induced gamma rays by inelastic scattering and capture reactions are summed in the same spectrum.

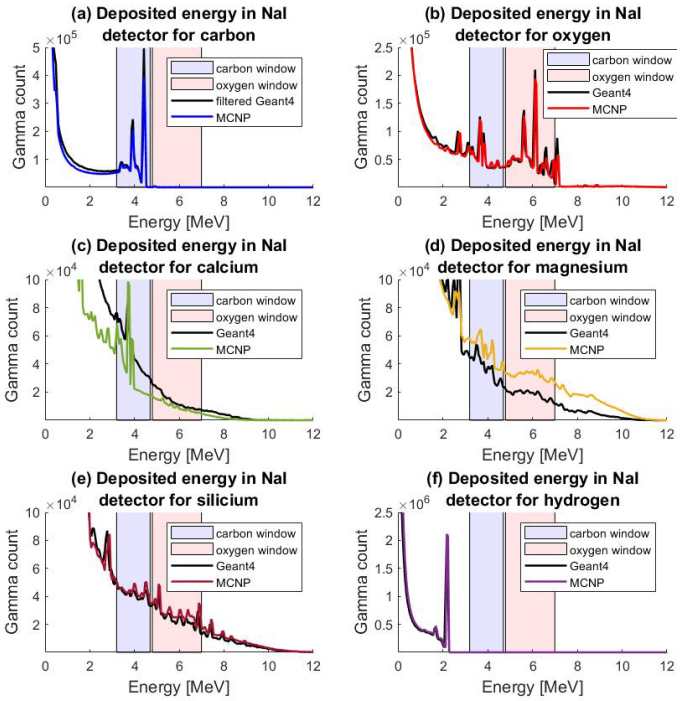

Fig. 10. Simulated neutron-gamma measurement spectra with a spherical model, a 14 MeV pulsed neutron source, an NaI detector and six pure chemical elements. Five materials at density 2.71 g/cm3 (carbon; oxygen; calcium; magnesium; silicon) and because of its large cross section, one material at density 0.5 g/cm3 (hydrogen) have been simulated. Graph (a) shows one MCNP spectrum (in blue) and two GEANT4 spectra, one without modification of the code (dotted black line) and one with a modified code to filter induced gamma rays (see text, black line).

Tables VII and VIII give total counts integrated in the oxygen and carbon windows and show maximum discrepancies of

37.4% with calcium in the carbon window and 42.6% with magnesium in the oxygen window.

MCNP and GEANT4 results for the hydrogen spectrum agree for energies below 2.2 MeV, but the number of counts in the C and O windows of interest is not relevant, similarly as the counts in the oxygen window of the carbon spectrum. Adding a filter on induced gamma creation process after inelastic interaction with carbon yield to decrease the discrepancies between MCNP and GEANT4 from 25.8% to 16.6% in the carbon window on the carbon spectrum. The main count deviations come from calcium and magnesium continuums in both windows which are not as easy to correct as for the carbon spectrum.

TAB. VII. TABLE OF OXYGEN WINDOW TOTAL COUNTS INTEGRATED ON NEUTRON-GAMMA MEASUREMENTS SPECTRA IN A SPHERICAL MODEL FOR SIX PURE ELEMENTS.

Neutron-Gamma C/O measurements NEAR detector in O window				
	Oxygen	Calcium	Magnesium	Silicium
Counts MCNP	2216955	426623	1365249	1221792
Counts GEANT4	2281493	593007	783742	1061198
GEANT4/MCNP	2,9%	39,0%	42,6%	13,1%

TAB. VIII. TABLE OF CARBON WINDOW TOTAL COUNTS INTEGRATED ON NEUTRON-GAMMA MEASUREMENTS SPECTRA IN A SPHERICAL MODEL FOR SIX PURE ELEMENTS.

Neutron-Gamma C/O measurements NEAR detector in C window			
	Carbon filtered	Carbon unfiltered	Oxygen
Counts MCNP	2319258	2319258	1432222
Counts GEANT4	2705439	2917505	1471031
GEANT4/MCNP	16,7%	25,8%	2,7%

Neutron-Gamma C/O measurements NEAR detector in C window			
	Calcium	Magnesium	Silicium
Counts MCNP	1001319	1357499	1217088
Counts GEANT4	1375929	1020289	1145298
GEANT4/MCNP	37,4%	24,8%	5,9%

Figure 11 shows six neutron-gamma C/O measurements spectra of a generic logging tool with two detectors (NEAR and FAR) in a well with 200 mm diameter and for three rock compositions.

Tables IX and X give the total counts integrated in the carbon and oxygen windows, showing maximum discrepancies of 64.8% for the NEAR detector and 110.3% for the FAR detector in the carbon window, 11.5% for the NEAR detector and 9% for the FAR detector in the oxygen window.

TABLE IX. TABLE OF CARBON WINDOW COUNTS INTEGRATED ON NEUTRON-GAMMA MEASUREMENTS SPECTRUMS OF A C/O GENERIC LOGGING TOOL WITH TWO DETECTORS IN THREE ROCK COMPOSITIONS AT 20 PU.

Neutron-Gamma C/O measurements NEAR detector in C window			
	Limestone	Sandstone	Dolomite
Counts MCNP	389	680	395
Counts GEANT4	641	581	597
GEANT4/MCNP	64,8%	14,7%	51,0%

Neutron-Gamma C/O measurements FAR detector in C window			
	Limestone	Sandstone	Dolomite
Counts MCNP	226	439	213
Counts GEANT4	476	411	382
GEANT4/MCNP	110,3%	6,4%	79,1%

TABLE X. TABLE OF OXYGEN WINDOW COUNTS INTEGRATED ON NEUTRON-GAMMA MEASUREMENTS SPECTRUMS OF A C/O GENERIC LOGGING TOOL WITH TWO DETECTORS IN THREE ROCK COMPOSITIONS AT 20 PU.

Neutron-Gamma C/O measurements NEAR detector in O window			
	Limestone	Sandstone	Dolomite
Counts MCNP	448	605	461
Counts GEANT4	420	536	444
GEANT4/MCNP	6,2%	11,5%	3,7%

Neutron-Gamma C/O measurements FAR detector in O window			
	Limestone	Sandstone	Dolomite
Counts MCNP	239	352	242
Counts GEANT4	260	322	236
GEANT4/MCNP	9,0%	8,5%	2,6%

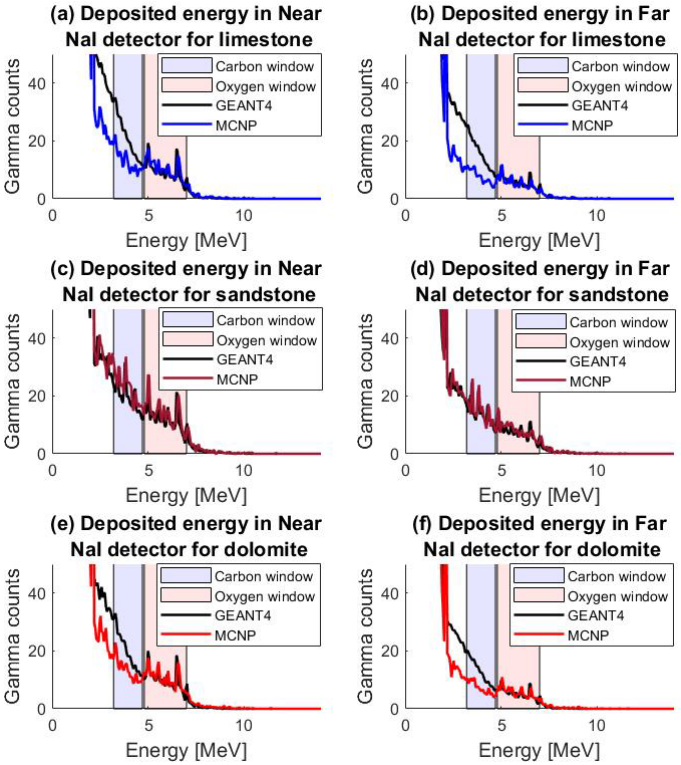

Fig. 11. Simulated neutron-gamma measurement spectra with a neutron-gamma C/O generic logging tool model, a 14 MeV pulsed neutron source, two NaI detectors and three different rocks at 20 pu (porosity unit): a 2.368 g/cm3 limestone (graphics a and b), a 2.323 g/cm3 sandstone (graphics c and d), and a 2.496 g/cm3 dolomite (graphics e and f).

Using the particle tracking of GEANT4, the nuclei that gave birth to the detected gamma rays in the C and O windows of interest can be identified. Induced gamma rays come from interactions between neutrons and calcium or oxygen nuclei, for more than 79% in a 20 pu limestone (cf. figure 11 a, b) and 62% in a 20 pu dolomite (cf. figure 11 e, f). On the other hand, 85% of induced gamma rays come from interactions between neutrons and silicon or oxygen nuclei in a 20 pu sandstone (cf. figure 11 c, d). Calcium appears to be the major element responsible for induced gamma rays in limestone and, to a lesser extent, in dolomite. The larger deviations in the carbon window for the limestone or dolomite lithology, compared to sandstone, is consistent with the observations made with the spherical model that calcium is the element showing the largest discrepancies between MCNP and GEANT4 (cf. figure 10 c and table VIII).

The overall agreement between GEANT4 and MCNP for neutron-gamma physics depends on the chemical composition and ranges of energies. It is excellent for a lithology like sandstone with discrepancies under 15%, but not acceptable for others such as limestone and dolomite in the carbon window.

VI. CONCLUSIONS

The comparison of GEANT4 and MCNP for simulating nuclear measurements shows a good agreement for gamma-gamma physics. Neutron-neutron physics also agrees quite satisfactorily between the two codes when molecular effects and proper neutron models are implemented. However, misfits appear for the neutron-gamma physics for some chemical compositions and energy ranges. Some local corrections in GEANT4, such as energy pass band filters on induced gamma rays, can improve the final spectra (e.g. in the case of carbon). The ultimate confirmation would come from experimental measurements that, at the same time, would also validate the concept of sensitivity functions to be used for multiphysics inversion applied to "Cased Hole" wellbore interpretation [14][15][16][17]. Ultimately, simulation results will be compared to experimental measurements in a calibration facility with real logging tools in various wellbore configurations (wells; casing; cement; formation), in view to definitely validate the concept of tool sensitivity functions [3].

REFERENCES

[1] C.J. Werner, et al., "MCNP6.2 Release Notes", Los Alamos National Laboratory, report LA-UR-18-20808 (2018).
[2] C.J. Werner (editor), «MCNP Users Manual - Code Version 6.2», LA-UR-17-29981 (2017).
[3] Chuilon, P., et al, 2019, From Houston API Calibration Pits… to Artigueloutan Logging Metrological Facility, Society of Petrophysicists and Well-Log Analysts, SPWLA 60th Annual Logging Symposium, June 15–19,SPWLA-2019-GGGGG, DOI: https://doi.org/10.30632/T60ALS-2019_GGGGG.
[4] EDGE—SpaceSuite, Apr. 2019, [online] Available: https://www.space-suite.com/edge/.
[5] El Kanawati, Wassila & Perot, Bertrand & Carasco, C. & Eleon, C. & Valkovic, Vladivoj & Sudac, Davorin & Obhodas, Jasmina & Sannie, G. (2011). Acquisition of prompt gamma-ray spectra induced by 14 MeV neutrons and comparison with Monte Carlo simulations. Applied radiation and isotopes : including data, instrumentation and methods for use in agriculture, industry and medicine. 69. 732-43. 10.1016/j.apradiso.2011.01.010.
[6] Ellis, D. V., Case, C. R. and Chiaramonte, J. M. (2003) 'Tutorial - Porosity from Neutron Logs I - Measurement', Petrophysics - The SPWLA Journal of Formation Evaluation and Reservoir Description, 44(06).
[7] Ellis, D. V., Case, C. R. and Chiaramonte, J. M. (2004) 'Tutorial - Porosity from Neutron Logs II - Interpretation', Petrophysics - The SPWLA Journal of Formation Evaluation and Reservoir Description, 45(01).
[8] FIRESTONE, R. B., & SHIRLEY, V. S. (1996). Table of isotopes. New York, Wiley.
[9] GangLi, GhaoutiBentoumi, ZinTun, LiqianLi, and BhaskarSur. APPLICATION OF GEANT4 TO THE DATA ANALYSIS OF THERMAL NEUTRON SCATTERING EXPERIMENTS. CNL Nuclear Review. 7(1): 11-7. https://doi.org/10.12943/CNR.2017.00002.
[10] GEANT4 - A Simulation Toolkit, S. Agostinelli et al., Nucl. Instrum. Meth. A 506 (2003) 250-303.
[11] Goodyear, G., Sood, A., Andrews, M., Solomon, C.J., Luycx, M., and Torres-Verdín, C., 2018, What's New in Borehole Nuclear Modeling? (A Lot!), Paper AAAA, Transactions, SPWLA 59th Annual Logging Symposium, 2–6 June, London, UK.
[12] Kavetskiy, Aleksandr & Yakubova, Galina & Prior, Stephen & Torbert, H.. (2017). Neutron-Stimulated Gamma Ray Analysis of Soil. 10.5772/68014.
[13] Knoll, G. F. (2010).
[14] Luycx, M. et al. (2020) 'Simulation of Borehole Nuclear Measurements: A Practical Tutorial Guide for Implementation of Monte Carlo Methods and Approximations Based on Flux Sensitivity Functions', Petrophysics - The SPWLA Journal of Formation Evaluation and Reservoir Description, 61(01), pp. 4–36. doi: 10.30632/PJV61N1-2020T1.
[15] Mendoza, A., C. Torres-Verdín, and W. E. Preeg, 2007, Rapid simulation of borehole nuclear measurements based on spatial flux-scattering functions: Presented at SPWLA 48th Annual Logging Symposium, O.
[16] Mendoza, A., C. Torres-Verdín, and W. E. Preeg, 2010a, Linear iterative refinement method for the rapid simulation of borehole nuclear measurements: Part 1 — Vertical wells: Geophysics, 75, no. 1, E9–E29, doi: 10 .1190/1.3267877.
[17] Mendoza, A., C. Torres-Verdín, and W. E. Preeg, 2010b, Linear iterative refinement method for the rapid simulation of borehole nuclear measurements: Part 2 — High-angle and horizontal wells: Geophysics, 75, no. 2, E79–E90, doi: 10.1190/1.3335953.
[18] Mendoza, E., Cano-Ott, D., Update of the Evaluated Neutron Cross Section Libraries for the GEANT4 Code, IAEA technical report INDC(NDS)-0758, Vienna, 2018.
[19] Perot, Bertrand & El Kanawati, Wassila & Carasco, C. & Eleon, C. & Valkovic, Vladivoj & Sudac, Davorin & Obhodas, Jasmina & Sannie, G. (2011). Quantitative comparison between experimental and simulated gamma-ray spectra induced by 14 MeV tagged neutrons. Applied radiation and isotopes : including data, instrumentation and methods for use in agriculture, industry and medicine. 70. 1186-92. 10.1016/j.apradiso.2011.07.005.
[20] Perot, Bertand & Carasco, C. & Bernard, S & Mariani, A & Szabo, J.-L & Sannie, G Valkovic, Vladivoj & Sudac, Davorin & Viesti, G & Lunardon, Matteo & Botosso, C & Nebbia, G. & Pesente, Silvia & Moretto, Sandra & Zenoni, Aldo & Donzella, Antonietta & Moszynski, Marek & Gierlik, Michał & Klamra, W & Salvato, M. (2008). Measurement of 14 MeV neutron-induced prompt gamma-ray spectra from 15 elements found in cargo containers. Applied radiation and isotopes : including data, instrumentation and methods for use in agriculture, industry and medicine. 66. 421-34. 10.1016/j.apradiso.2007.11.011.
[21] Simakov, S P, Pavlik, A, Vonach, H, and Hlavac, S. Status of experimental and evaluated discrete {gamma}-ray production at E{sub n}=14.5 MeV. Final report of Research Contract 7809/RB, performed under the CRP on measurement, calculation and evaluation of photon production data. IAEA: N. p., 1998. Web.
[22] Trouche*, A.,* et al., "EDGE: new GDML CAD tool for GEANT4 based analysis and interoperability bridge for high-energy particle modelling tools", ENSAR2 workshop: GEANT4 in nuclear physics – 24-26 April 2019 – Madrid (Spain).
[23] Velker, Nikolay & Banzarov, Bair & Inanc, Feyzi & Simonov, Nikolai. (2012). GEANT4 for Solving Nuclear Geophysics Problems (Russian). 10.2118/162008-RU.